Supplementary figures

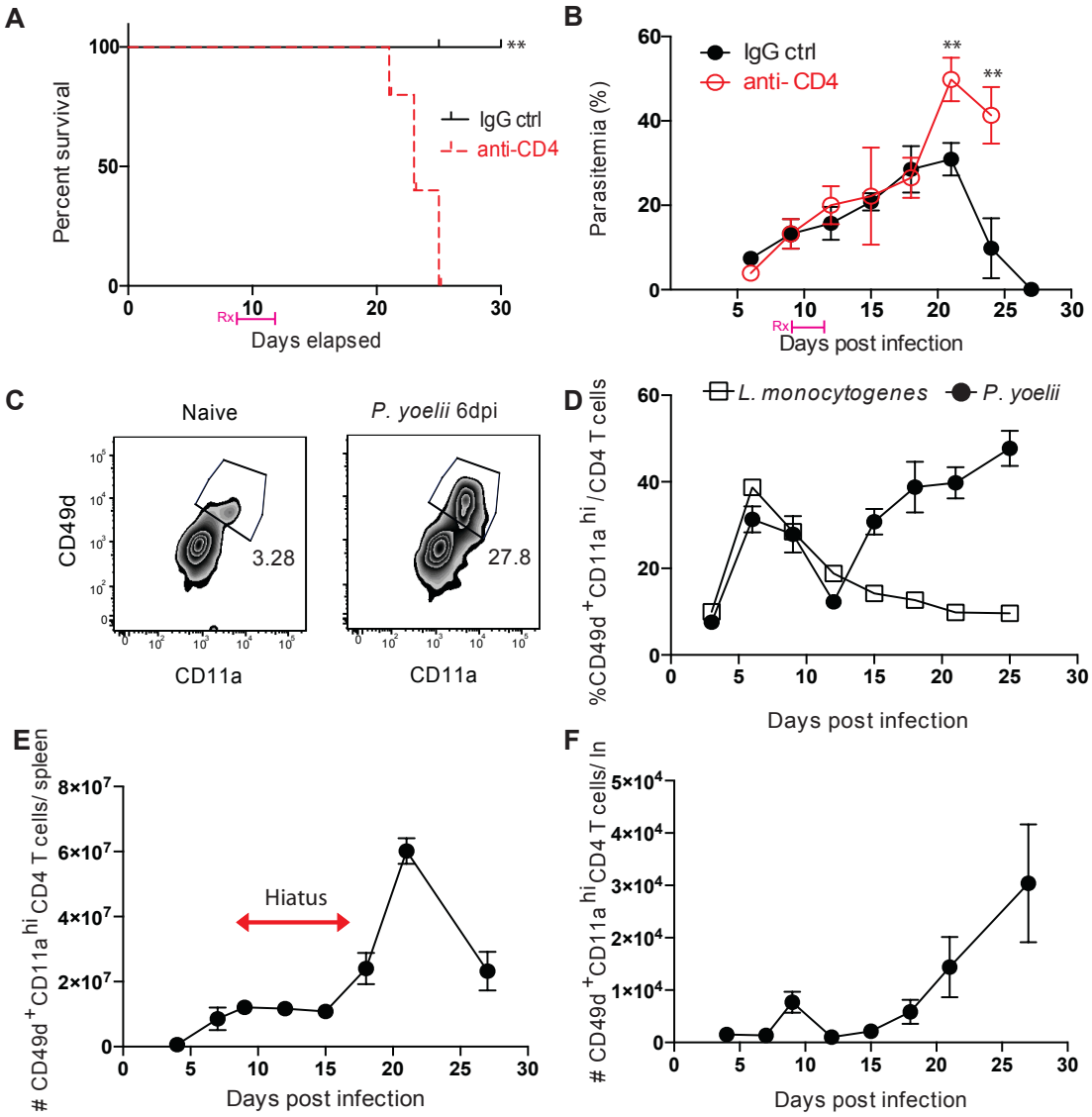

Supplementary figure 1: Helper T cells are critical in control of mouse malaria, but exhibit atypical kinetics of response to infection.
(A-B) Kinetics of survival (A) and parasitemia (B) in *Py* 17XNL infected C57BL/6 mice with or without CD4 T cell depletion on days 9 and 11 post infection (red line). (C-F) Representative flow plots showing surrogate markers ($CD11a^{hi}$, $CD49d^{+}$) for activated, pathogen-specific CD4 T cells in blood in a naïve or *Py* 17XNL infected mouse (C). Numbers represent frequencies in blood (D) or absolute numbers in spleen or lymph nodes (E-F) of pathogen-specific CD4 T cells after *L. monocytogenes* (D) or *Py* (D-F) infections in C57BL/6 mice. All data represent 1 of 3 separate experiments, each with at least 5 mice per group and error bars represent mean $\pm$ s.e.m. ** indicates $P \leq 0.01$ comparing the treatment and control groups using chi square (A) or two-tailed student t-tests (B).

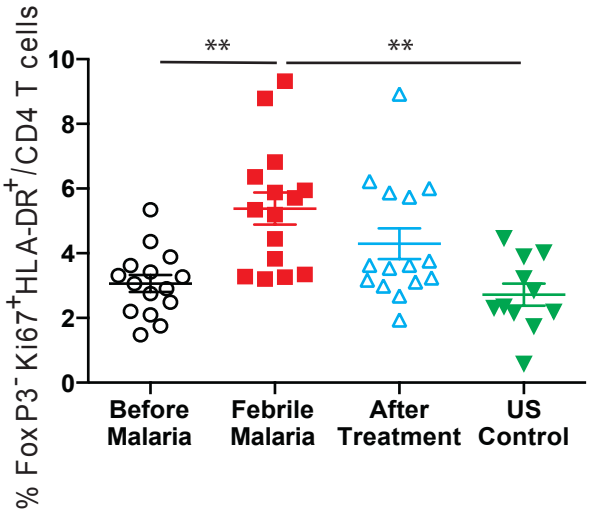

Supplementary figure 2: Helper T cells expand during malaria in humans. Frequency of activated non-Treg CD4 T cells in PBMCs in a cohort of children in Mali before, during and after acute febrile malaria, compared to that of healthy controls in the United States. Each data point indicates a subject and error bars represent mean $\pm$ s.e.m. * or ** indicates $P \leq 0.05$ or 0.01 respectively comparing the indicated groups using one-way ANOVA with Tukey's correction ($F_{3,52}=8.31$).

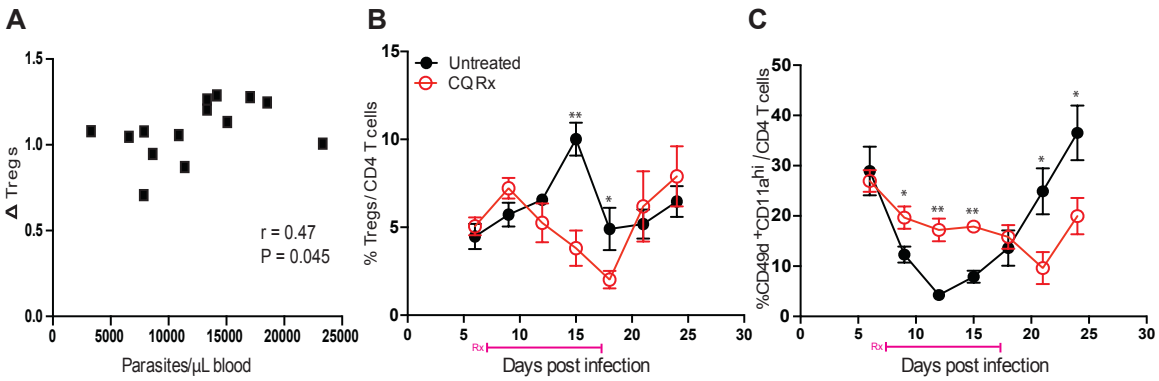

Supplementary figure 3: Treg frequencies positively correlate with parasite densities in blood and restrained Th cell expansion.
(A)Spearman rank correlation between parasitemia and fold change in Tregs during acute febrile malaria, in a cohort of children in Mali. (B-C) Kinetics of Foxp3^{+} regulatory (B) or activated Th (C) cell frequencies in circulation of *Py* infected C57BL/6 mice treated with or without a subtherapeutic dose of chloroquine (CQ). Data represent 1 of 3 separate experiments, each with at least 5 mice per group and error bars represent mean $\pm$ s.e.m. * or ** indicates P$\leq$ 0.05 or 0.01 respectively comparing the treatment and control groups using two-tailed student t-tests at the indicated time points.

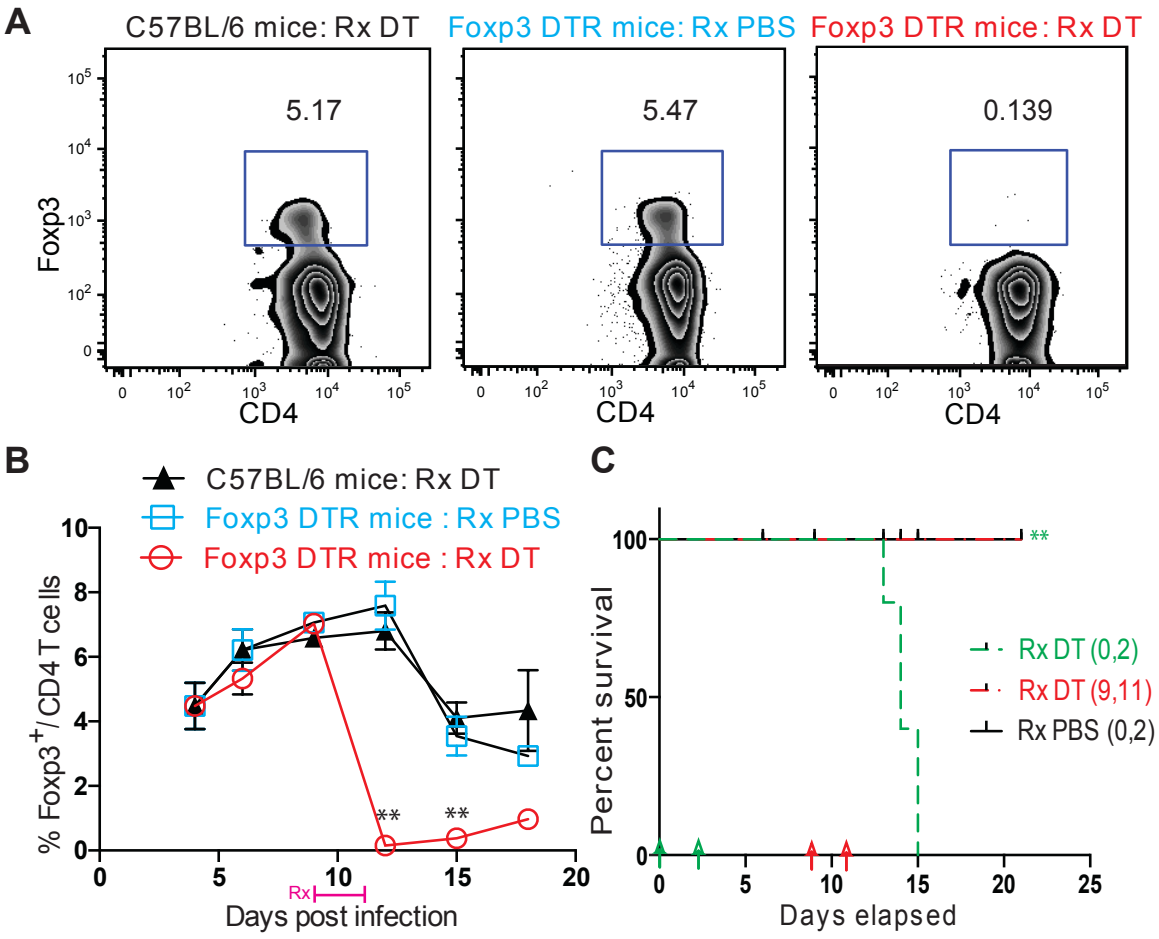

Supplementary figure 4: Regulatory T cell depletion in malaria infected Foxp3-DTR mice treated with diphtheria toxin.

(A) Representative flow plots from 12dpi showing frequencies of Foxp3$^+$ regulatory T cells in the blood of C57BL/6 or Foxp3 DTR mice infected with *Py* and treated with DT (Rx DT) or PBS control (Rx PBS) on days 9 and 11 post infection. (B) Kinetics of Foxp3$^+$ regulatory T cell frequencies in (A). Survival curve in Foxp3 DTR mice infected with *Py* and treated with DT (Rx DT) or PBS control (Rx PBS) on days 0 and 2 or 9 and 11 post infection. All Data represent 1 of 2 separate experiments with 3-5 mice per group, error bars represent mean $\pm$ s.e.m and ** indicates $P \leq 0.01$ comparing the Foxp3 DTR: RxDT and Foxp3 DTR: Rx PBS groups with two-way ANOVA and Tukey's correction, at the indicated time points (B; $F_{2,60}=21.60$) or Mantel-Cox Chi square test (C).

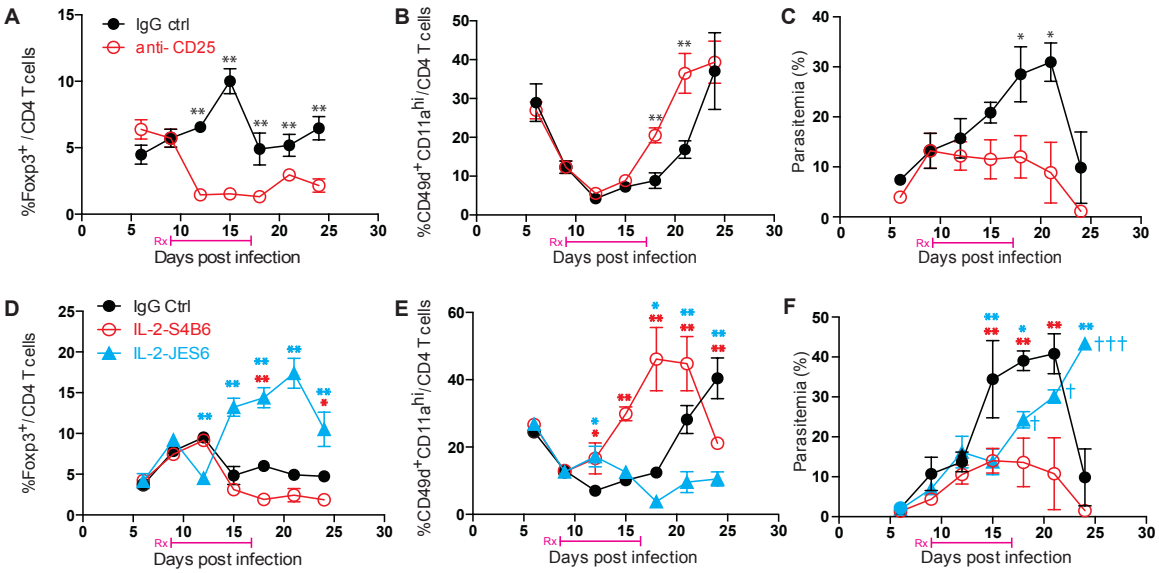

Supplementary figure 5: Regulatory T cells control helper T cell responses and immunity to malaria.

(A-C) Frequencies of Foxp3$^+$ regulatory T cells (A), activated CD4 T cells (B) and the frequency of infected RBCs (C) in C57BL/6 mice at various time points post infection with *Py* and treatment from days 9-16 (red bars) with anti-CD25 antibodies or control IgG as indicated. (D-F) Frequencies of Foxp3$^+$ regulatory T cells (D), activated CD4 T cells (E) and the frequency of infected RBCs (F) in C57BL/6 mice at various time points post infection with *Py* and treated from days 9-16 (red bars) with IL-2-S4B6 complex, IL-2-JES6 complex or control IgG as indicated. Data represent 1 of 3 separate experiments with 5 mice per group and presented as mean $\pm$ s.e.m. Color coded * or ** indicate $P \leq 0.05$ or 0.01 respectively, comparing the corresponding treatment and control groups using two-tailed student t-tests (A-C) or two-way ANOVA with Tukey's correction (D: $F_{2,77}=87.56$, E: $F_{2,77}=48.30$ and F: $F_{2,77}=62.17$). † indicates the death of one mouse in the corresponding group.

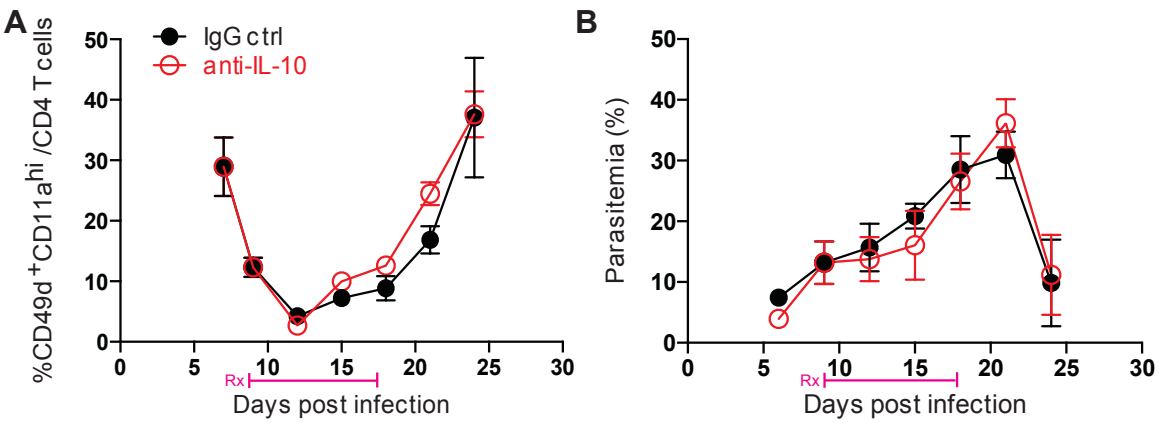

Supplementary figure 6: Neutralizing IL-10 does not alter helper T cell responses or immunity to mouse malaria

Frequencies of activated CD4 T cells (A) and frequency of infected RBCs (B) in C57BL/6 mice at various time points post infection with *Py*. Infected mice were treated from days 9-16 (red bars) with IL-10 neutralizing antibody or control IgG as indicated, in extended figure 4. Data represent 1 of 2 separate experiments, with 5 mice per group and is presented as mean $\pm$ s.e.m.

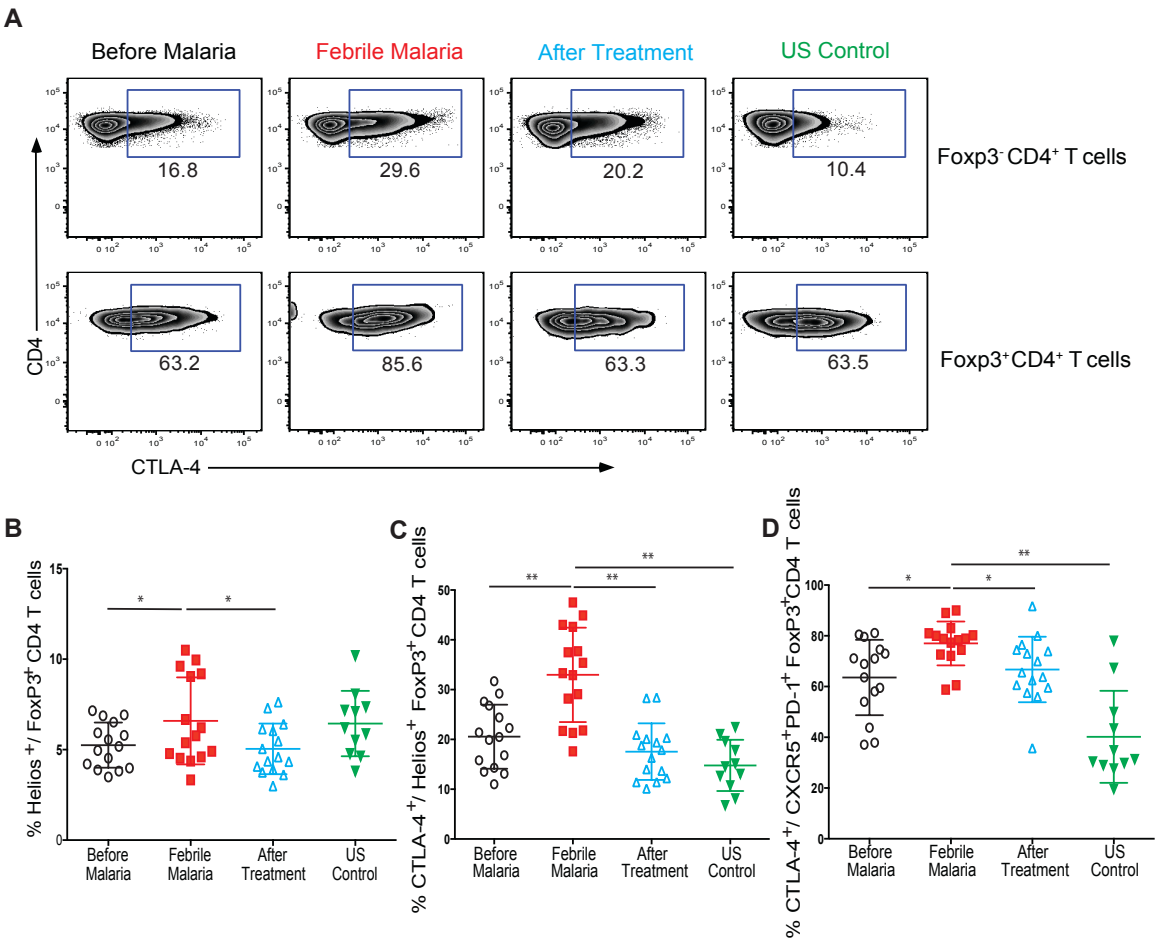

Supplementary figure 7: CTLA-4 expression and frequencies of various suppressive T cell subsets augmented in human malaria.
(A) Representative flow plots indicating the frequencies of CTLA-4 expressing Th cells and Tregs in a cohort of children in Mali before, during and after acute febrile malaria, compared to healthy controls. (B-D) Frequencies of Helios$^+$ Tregs (B), CTLA4$^+$ Helios$^+$ Tregs (C) or CTLA-4$^+$ follicular Tregs (D) in PBMCs in a cohort of children in Mali before, during and after acute febrile malaria, compared to that of healthy controls in the United States. Each data point indicates a subject and error bars represent mean $\pm$ s.e.m. * or ** indicates P $\leq$ 0.05 or 0.01 respectively comparing the indicated groups using one-way ANOVA with Tukey's correction (B: $F_{1.4,19}$=9, C: $F_{3,52}$=18.37, D: $F_{3,52}$=15.74).

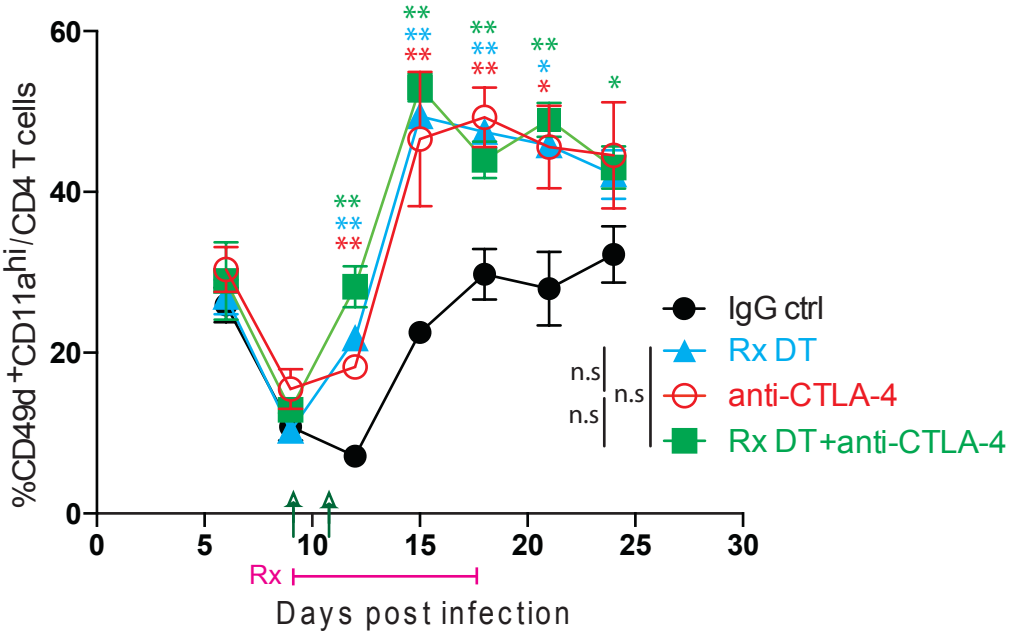

Supplementary figure 8: CTLA-4 blockade under Treg depletion does not further alter the kinetics of Th cell responses in malaria.
Frequencies of activated CD4 T cells in C57BL/6 mice at various time points post infection with *Py* and treated with DT (9 and 11dpi, green arrows) and/or anti-CTLA-4 or control IgG as in Figure 3 (A). Data represent 1 of 2 separate experiments, each with 5 mice per group and is presented as mean ± s.e.m. Color coded * or ** indicate $P \leq 0.05$ or 0.01 respectively, comparing the corresponding treatment and IgG control groups using two-way ANOVA with Tukey's correction; $F_{3,93}=42.78$. n.s indicates $P > 0.05$.

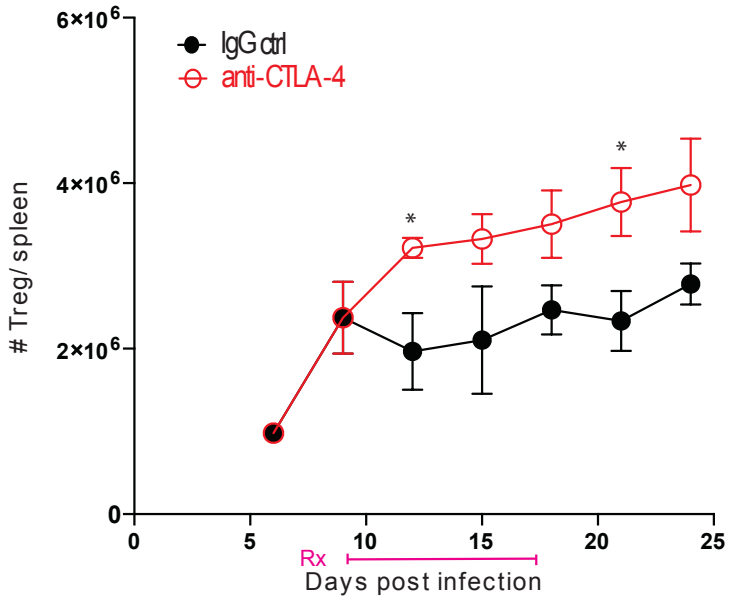

Supplementary figure 9: CTLA-4 blockade does not deplete Tregs after Py infection.

Total numbers of Foxp3^{+}CD4^{+} Treg cells in spleen at various time points post *Py* infection in C57BL/6 mice with or without CTLA-4 blockade as in Figure 3(A). Data presented as mean $\pm$ s.e.m at each time point or sera dilution and represent 1 of 3 separate experiments, each with at least 5 mice per group. * indicates P$\leq$ 0.05 respectively, comparing the treatment and control groups at the indicated time points with two-tailed student t-tests.

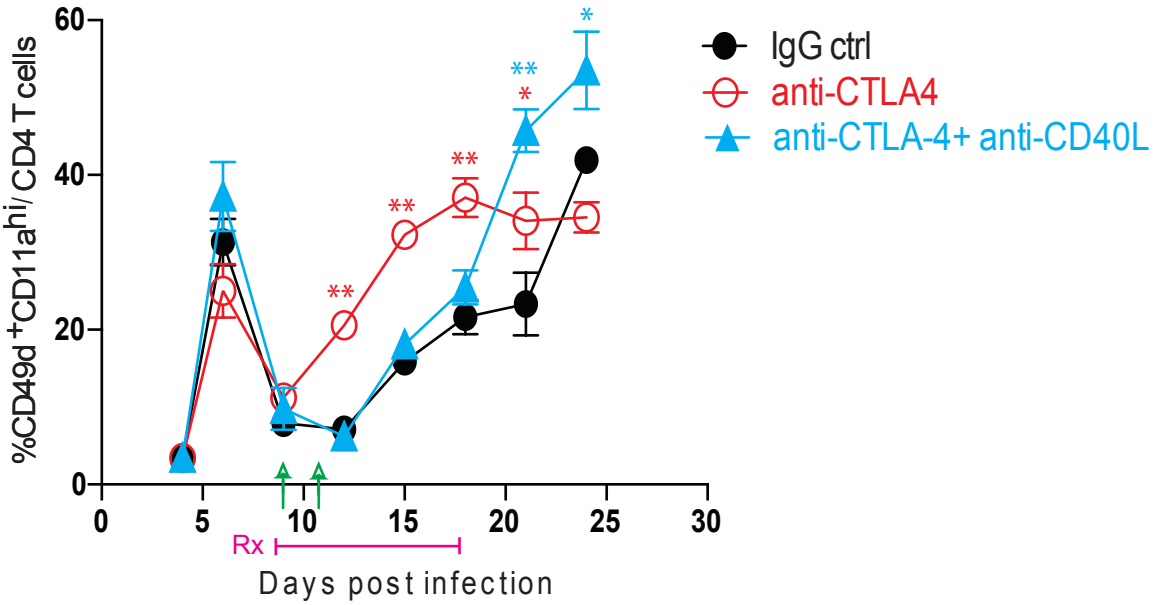

Supplementary figure 10: GC B cell depletion stalls the recovery of CD4 T cell responses after CTLA-4 blockade in malaria.
Frequencies of activated CD4 T cells in C57BL/6 mice at various time points post infection with *Py* and treated with anti-CD40L (9 and 11dpi, green arrows) and/or anti-CTLA-4 or control IgG as in Figure 3 (A). Data represent 1 of 2 separate experiments, each with 5 mice per group and is presented as mean $\pm$ s.e.m. Color coded * or ** indicate $P \leq 0.05$ or 0.01 respectively, comparing the corresponding treatment and IgG control groups using two-way ANOVA with Tukey's correction; $F_{3,114}=10.03$.

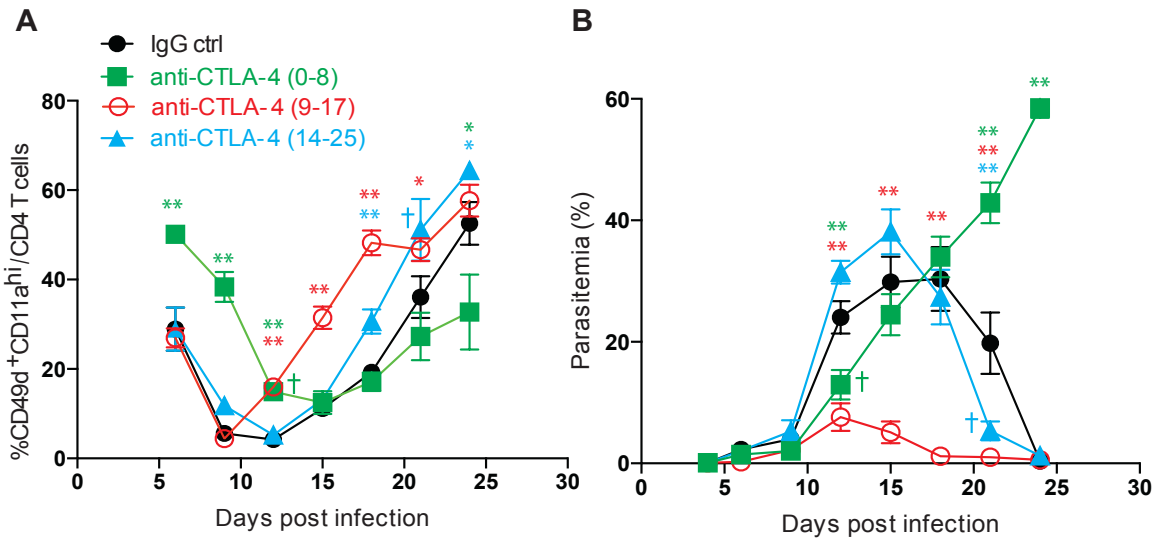

Supplementary figure 11: CTLA-4 blockade coinciding with the expansion of Tregs and the Th cell hiatus is critical to control malaria.
Frequencies of activated CD4 T cells (A) or parasitemia (B) in circulation in C57BL/6 mice at various time points post infection with *Py* and treated every other day, with anti-CTLA-4 or control IgG during the indicated time-window. Data compiled from 3 separate experiments, each with 5 mice per group and is presented as mean ± s.e.m. Color coded * or ** indicate $P \leq 0.05$ or 0.01 respectively, comparing the corresponding treatment and IgG control groups using two-way ANOVA with Tukey's correction (A: $F_{3,105}=13.89$, B: $F_{3,105}=89.14$). † indicates the death of one mouse in the corresponding color coded group.

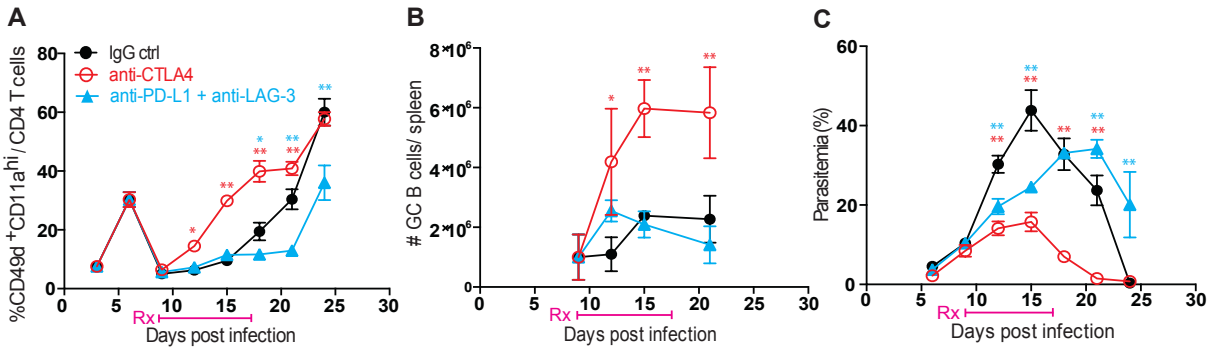

Supplementary figure 12: PD-L1/ LAG-3 blockade during the hiatus in Th cell response does not enhance immunity to malaria

Frequency of activated CD4 T cells in blood (A), total $CD95^{+}GL7^{+}CD19^{+}B220^{+}$GC B cells in spleen (B) and the frequency of infected RBCs (C) in C57BL/6 mice at various time points post infection with *Py* and treatment from days 9-17 with anti-CTLA-4, anti PD-L1/LAG-3 antibodies or control IgG as indicated. Data represent 1 of 2 separate experiments with 5 mice per group and presented as mean $\pm$ s.e.m. Color coded * or ** indicate $P \leq 0.05$ or 0.01 respectively, comparing the corresponding treatment and IgG control group using two-way ANOVA with Tukey's correction (A: $F_{3,12}=45.36$, B: $F_{3,6}=40.14$, C: $F_{3,12}=56.82$).

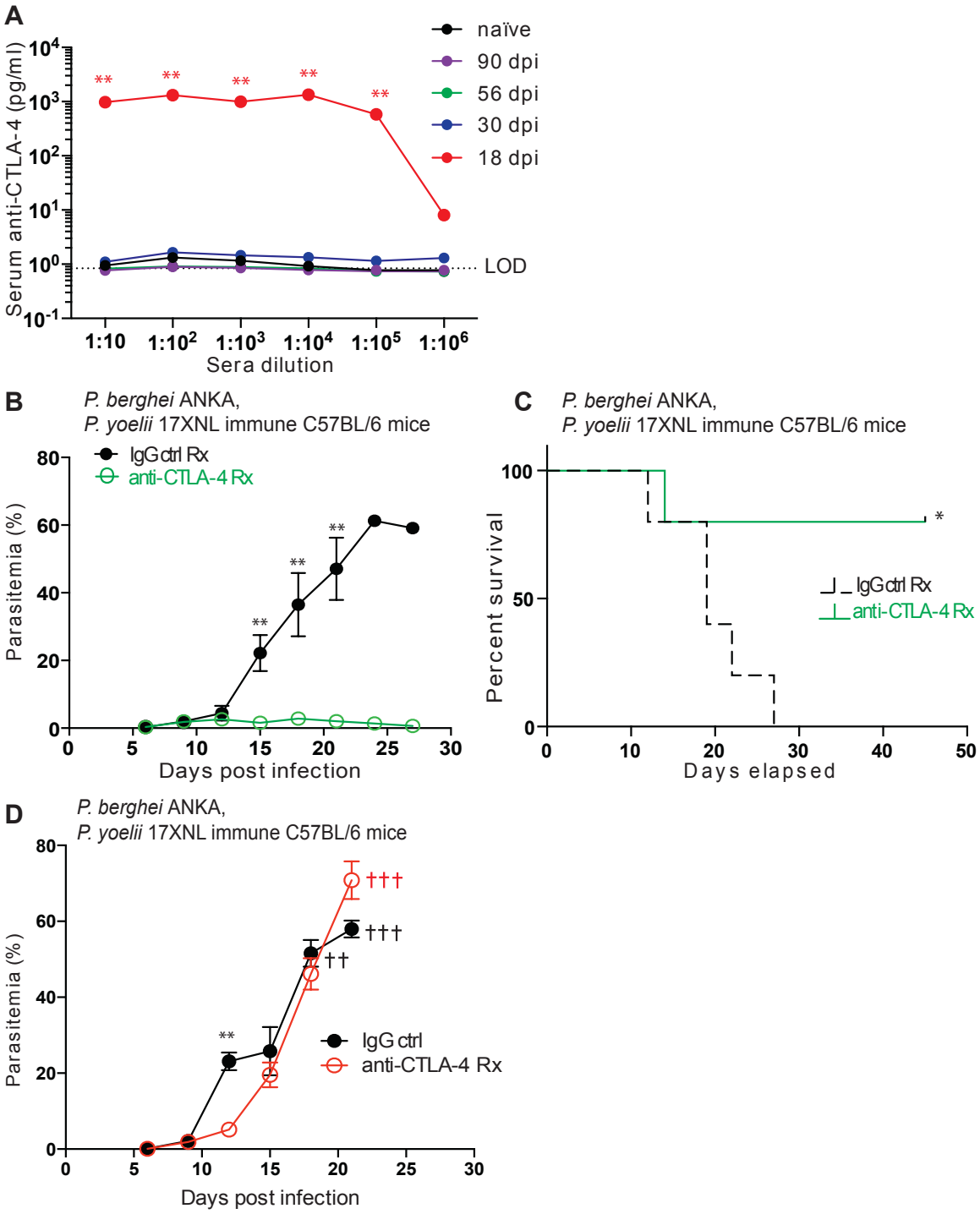

Supplementary figure 13: CTLA-4 blockade imparts durable, cross species, Th cell dependent immunity to blood-stage malaria

(A) Residual anti-CTLA-4 antibody in serum at various time points post *Py* infection in C57BL/6 mice treated with anti-CTLA-4 antibody, as in Figure 3(A), detected by ELISA. Data compiled from 2 biological replicates, where * or ** indicate $P \leq 0.05$ or 0.01 respectively, comparing the treatment and control

groups using two-way ANOVA with Dunnet's correction for multiple comparison. LOD indicates the limit of detection. (B-C) Parastiemia at the indicated time points (B) or survival (C) in mice treated as indicated in Fig 3(A), heterologously challenged with *P. berghei* at 110 dpi. (D) Frequency of infected RBC at the indicated time points in mice depleted of CD4 T cells prior to the heterologous *P. berghei* challenge above. Data represent 1 of 2 separate experiments, each started with 5 mice per group. Error bars represent s.e.m and *or **indicate $P \leq 0.05$ or 0.01 respectively, comparing the treatment and control groups at the indicated time points with two-tailed student t-tests (B, D) or Mantel-Cox chi-square test (C).

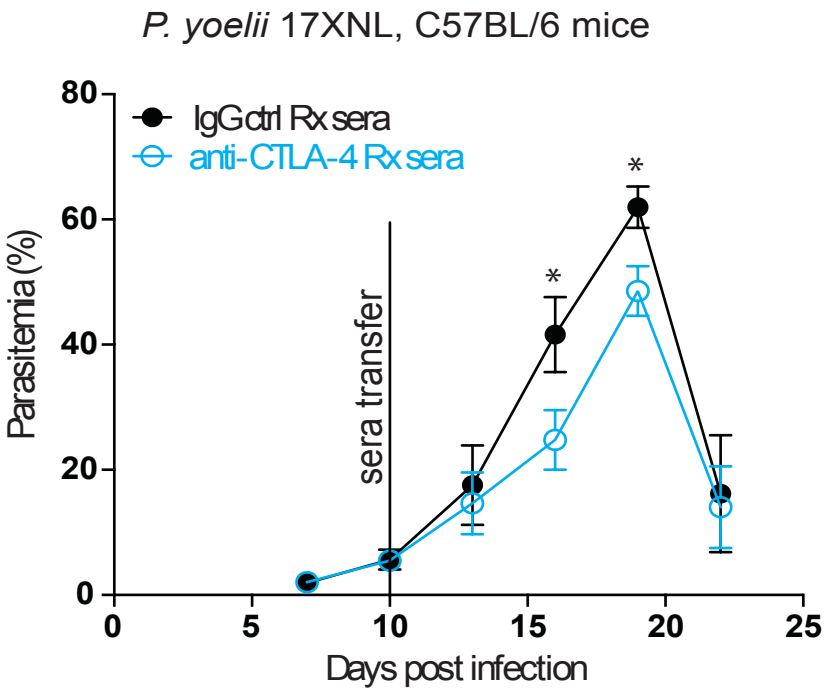

Supplementary figure 14: CTLA-4 blockade enhances passive humoral immunity to malaria.
Parasitemia at the indicated time points in *Py* infected C57BL/6 mice that received sera (100μl) at 10 dpi, obtained from donor mice in Figure 4(A), at 56 dpi. Data represent 1 of 2 separate experiments, each with 5 mice per group. Error bars represent s.e.m and * indicate $P \leq 0.05$, comparing the groups at the indicated time points with two-tailed student t-tests.

Supplementary Video S1: CD4 T:B cell clusters in splenic GCs of *Py* infected mice.
Immunofluorescence microscopy and 3D volumetric reconstruction of the splenic architecture showing T cell zones ($CD4^+$, pseudocolored green) B cell follicles ($B220^+$, pseudocolored blue), GC reaction ($GL7^+$, pseudocolored grey) and plasmablasts ($CD138^+$, pseudocolored red) from a C57BL/6 mouse inoculated with *Py*, 27dpi. Plasmablasts and CD4 T cell: B cell clusters within the GC are visible from 00:00:17s. Video representative of at least 5 regions observed in 9 sections examined from 3 separate mice from 3 separate experiments.

Supplementary Video S2: Tfh:B:Tfr cell clusters in splenic GCs of *Py* infected mice
Immunofluorescence microscopy and 3D volumetric reconstruction of the splenic GC and surrounding structures showing clusters of Tfh cells, B cells and Tfr cells seen the in the GC; from a C57BL/6 mouse infected and treated with anti-CTLA-4 as in Figure 2G, 15dpi. CD4 is pseudocolored green, B220 blue, Nrp-1 grey and CTLA-4 red. Video representative of at least 5 regions observed in 9 sections examined from 3 separate mice from 3 separate experiments.

Supplementary Video S3: Close apposition of B cells and Tfr cells in GCs of *Py* infected mice
Higher magnification Immunofluorescence microscopy and 3D volumetric reconstruction of splenic GC (represented in Fig 2G, middle panel) showing close apposition of B cells and Tfr cells from a *Py* infected C57BL/6 mouse infected, 21dpi. B220 is pseudocolored blue, Foxp3 grey and CTLA-4 red. Video representative of at least 5 regions observed in 9 sections examined from 3 separate mice from 3 separate experiments.

Supplementary Video S4: CTLA-4 on the B cell surface proximal to Tfr cell in a Tfh:B:Tfr cell cluster
Immunofluorescence microscopy and 3D volumetric reconstruction of a single Tfh:B:Tfr cell cluster showing B:Tfr cell interaction in the lymph node of a *Py* infected C57BL/6 mouse, 21dpi. B220 is pseudocolored blue, Nrp-1 grey and CTLA-4 red. Video representative of at least 5 regions observed in 9 sections examined from 3 separate mice from 3 separate experiments.

Supplementary Video S5: Tfr cells transiently interact with B cells in the splenic GCs of *Py* infected mice.
Intravital confocal immunofluorescence microscopy (total duration= 30 mins) of spleen in *Py* infected Foxp3-GFPx Bcl-6-RFP.B6 mice, 21 dpi. B220 is pseudocolored blue. Tfr cells ($Foxp3^+Bcl6^+$) appear yellow, B cells blue, GC B cells ($B220^+Bcl6^+$) magenta and Tfh cells ($B220^-Bcl6^+$) red. Video represents 1 of 12 different regions imaged in three separate mice.

Supplementary table 1: Demographics and parasitemia data of study subjects in the cohort.

Subject ID	Age (yrs)	Gender	Ethnicity	Before Malaria Parasitemia (Parasites/ uL blood)	Febrile Malaria Parasitemia (Parasites/ uL blood)
435	9	M	Bambara	0	10875
443	9	M	Bambara	0	N/A
453	9	F	Bambara	0	14175
461	8	F	Bambara	0	7850
467	8	M	Bambara	0	18525
512	7	F	Bambara	0	7875
517	7	M	Bambara	0	6575
523	6	M	Bambara	0	17050
548	6	M	Bambara	0	3300
554	5	M	Bambara	0	23325
566	5	M	Bambara	0	13325
575	5	M	Other	0	8625
576	5	M	Bambara	0	11400
581	4	M	Bambara	0	13325
583	4	M	Bambara	0	15075